The attempt for a microscopic mean field treatment of the Gay-Berne model and the mean field correction to the Pade formulas

Eleftherios Mainas

May 2022

1 Integrating the pair potential

In order to obtain a value for mean-field orientational correlation parameter ϵ we need to solve the following equation,

$$\epsilon = -\frac{1}{2}\rho_R \int d\vec{r} g_R(r;\rho_R,T_R) \sum_{n=2,4,...} n^2 \frac{1}{4} c_{nn}(r) \tag{1}$$

This equation is true for the large γ limit, $\gamma \to \infty$. The pair correlation function of the reference system will be solely defined by the potential energy of the reference system and its thermodynamic conditions ρ_R and T_R. The pair potential of the reference system, $u_R(r)$, is obtained from the small $\gamma \to 0$ limit. We simply integrate all the orientational degrees of freedom out of the Gay-Berne potential,

$$u_R(r) = \int \frac{d\hat{\Omega}_j}{2\pi} \int \frac{d\hat{\Omega}_k}{2\pi} u_{GB}(\vec{r}_{ij},\hat{\Omega}_j,\hat{\Omega}_k)$$

In a non-vector notation we write,

$$u_R(r) = \int_0^\pi \frac{d\theta_i}{\pi} \int_0^\pi \frac{d\theta_j}{\pi} u_{GB}(\vec{r}_{ij},\hat{\Omega}_i,\hat{\Omega}_j)$$

The orientation of each molecule j, θ_j, is defined by the angle of the orientational unit vector of the j-th molecule $\hat{\Omega}_j$ with respect to an arbitrary macroscopic axis $\hat{x}$,

$$\cos\theta_j = \hat{x} \cdot \hat{\Omega}_j$$

2 Integrating the pair potential

For the integration I used three different algorithms: Trapezoid, Simpson and Boole. The first one is the simplest but with the lowest accuracy and the last one is the slowest but with very high accuracy. When the number of intervals is $n = 20$ all three algorithms give similar curves.

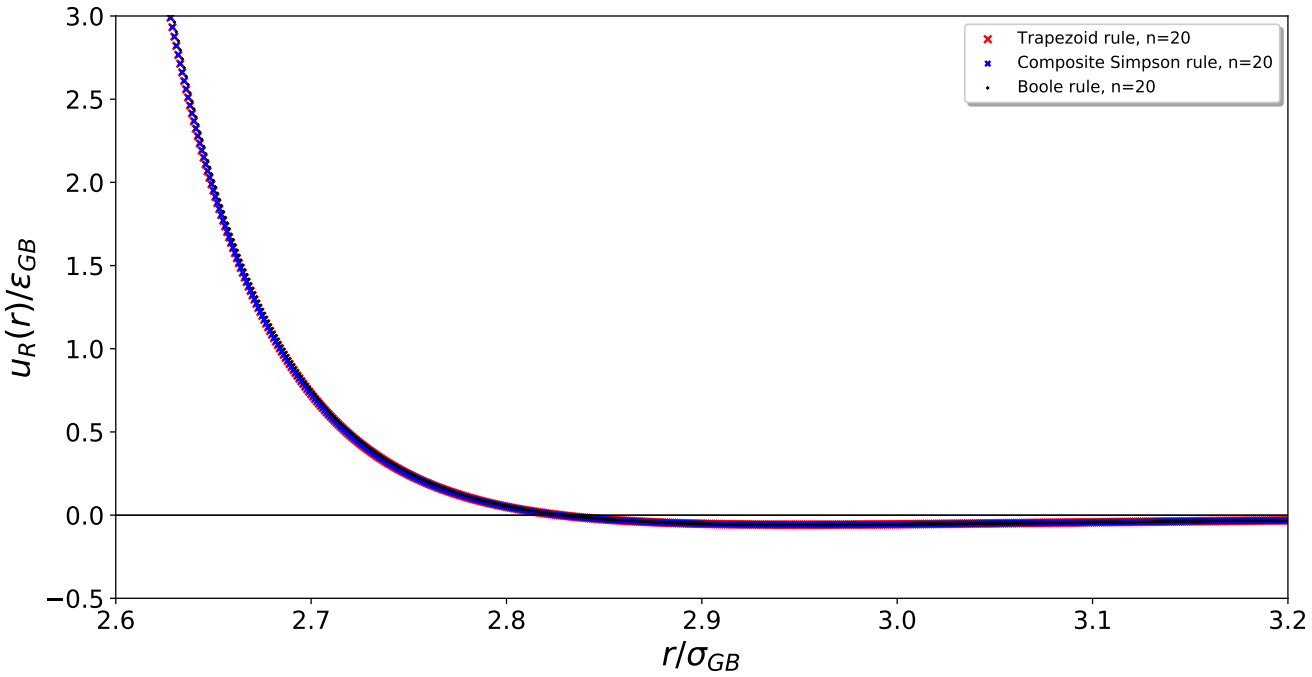

Figure 1: The pair potential energy of the reference system. I used a grid of 20×20 for the numerical integration. For comparison, at $r/\sigma_{GB} = 2.7$ the lowest accuracy algorithm (trapezoid) and the highest accuracy algorithm differ only by 3.4%. I think it is safe we use the trapezoid rule for the rest of the integrations and perhaps use more intervals.

From now on we will do numerical integrations with the trapezoid rule on a 200×200 grid. Let's now zoom in closer to the minimum part of the pair potential curve and see how we can define the new length and energy scale of the problem.

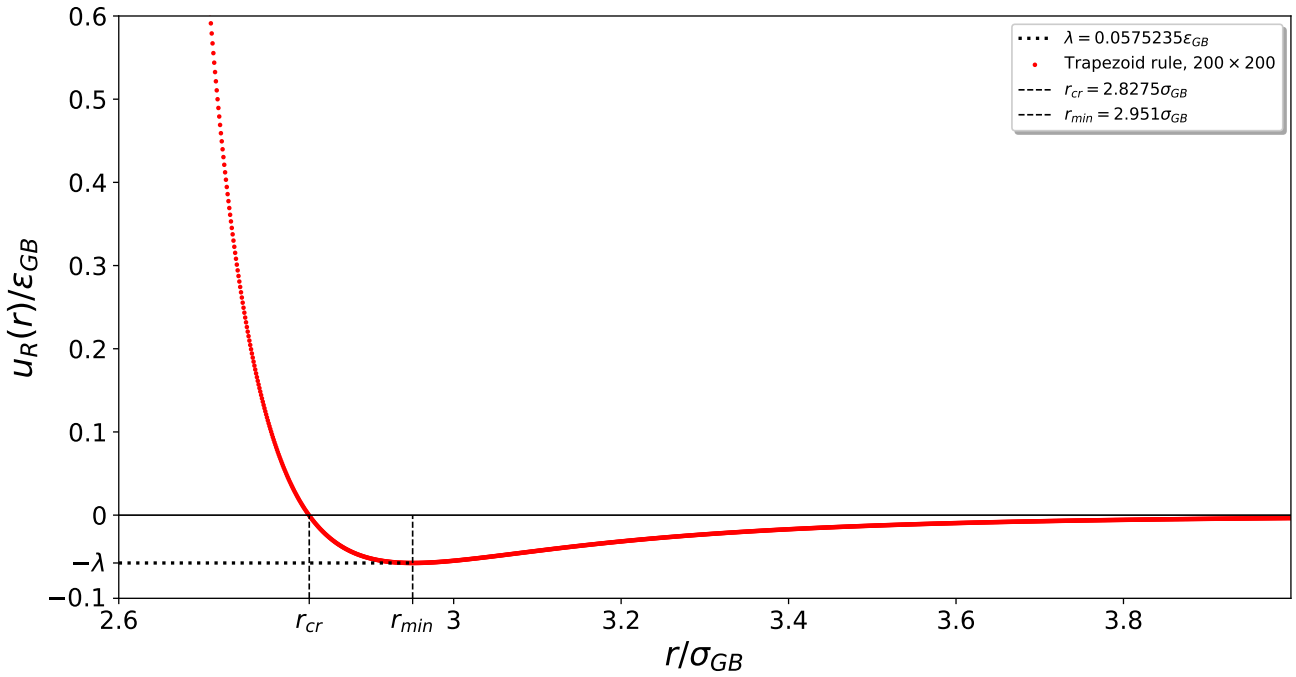

Figure 2: The pair potential energy of the reference system. The curve crosses the x-axis at $r_{cr} = 2.8275\sigma_{GB}$ and has a minimum of $u_R = -0.0575235\epsilon_{GB}$ at $r_{min} = 2.951\sigma_{GB}$. We may use these two facts to define the length and energy scale of the reference system.

In principle we could find λ and r_{min} by solving the equation

$$\frac{d(u_R(r)/\epsilon_{GB})}{dr}|_{r=r_{min}} = 0$$

$$\lambda = |u_R(r_{min})| \tag{2}$$

but we don't have an analytic function. Instead we have a list of points so I simply inspected the data and spotted the minimum. It should be very close to the exact answer. I did the same in order to find r_{cr},

$$u_R(r_{cr}) = 0 \tag{3}$$

We may use the variables λ and r_{cr} in order to define the effective size and energy scale of the reference system.

3 Fixing the scales

The first problem we need to solve is the calculation of the new length scale and new energy scale of the reference system. Since we have integrated all orientational degrees of freedom out of the pair potential, our reference system will have a much smaller density in terms of Gay-Berne scale and much different temperature in terms of Gay-Berne energy units. We can get the new scales from figure 2. The pair potential crosses the x-axis at $r_1 = 2.8275\sigma_{GB}$ and has a minimum of $u_0 = -0.0575235\epsilon_{GB}$. These two values define the new length and thermal scale of the problem. We have the reference density, ρ_R and the Gay-Berne density as ρ_{GB}. We wish the two reduced densities to be the same

$$\rho_R^* = \rho_{GB}^*$$

or

$$\rho_R \sigma_R^2 = \rho_{GB} \sigma_{GB}^2$$

From figure 2 we have

$$\sigma_R = r_{cr} = 2.8275\sigma_{GB}$$

and the density we used for the Gay-Berne simulation was

$$\rho_{GB} = 0.285$$

With these two facts in hand we get to the new density,

$$\boxed{\rho_R \sigma_{GB}^2 = \frac{0.285}{2.8275^2} = 0.035648}$$

Similarly for the temperature,

$$\epsilon_R = \lambda = 0.057524 \epsilon_{GB}$$

and

$$\frac{k_B T_{GB}}{\epsilon_{GB}} = 1$$

Again we say that the temperature in terms of the reference system energy scale needs to be the same as the Gay-Berne one

$$\frac{k_B T_R}{\epsilon_R} = \frac{k_B T_{GB}}{\epsilon_{GB}} = 1$$

The reference system temperature in terms of the Gay-Berne energy scale is

$$\boxed{\frac{k_B T_R}{\epsilon_{GB}} = 0.057524}$$

4 WCA decomposition of $u_R(r)$

From equation 2 we know, λ and r_{min} so we can use them to decompose the reference pair potential to a repulsive part

$$u_R^{repulsive} = \begin{cases} u_R(r) + \lambda, & r < r_{min} \\ 0, & r \geq r_{min} \end{cases}$$

and an attractive part

$$u_R^{attractive} = \begin{cases} -\lambda, & r \leq r_{min} \\ u_R(r), & r > r_{min} \end{cases}$$

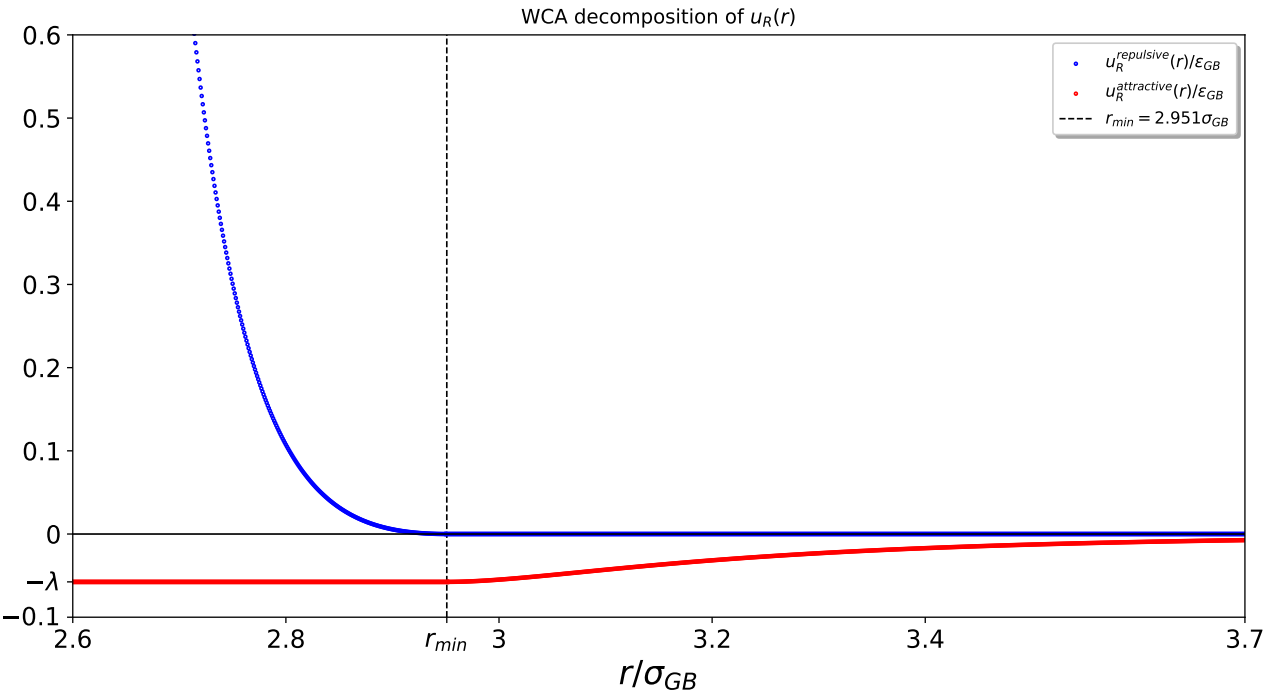

Figure 3: The decomposition of the pair reference potential to a repulsive part and an attractive part. The minimum is $r_{min} = 2.951\sigma_{GB}$ and $\lambda = 0.0575235\epsilon_{GB}$

We will need just the repulsive part in order to calculate the pair correlation function so we need to come up with a non-linear fit to the repulsive wall of the potential.

5 Non-linear fit

We can approximate the repulsive data,

$$u_R^{repulsive} = \begin{cases} u_R(r) + \lambda, & r < r_{min} \\ \\ 0, & r \geq r_{min} \end{cases}$$

with the following function

$$f(r) = \begin{cases} a[\exp\left(-(\frac{r}{b})\right) - \exp\left(-(\frac{r_{min}}{b})\right)], & r < r_{min} \\ \\ 0, & r \geq r_{min} \end{cases}$$

where the coefficients can be found through a simple least squares method,

$$a = 4.11842680 \times 10^{22} \quad \epsilon_{GB}$$

$$b = 0.0516268618 \quad \sigma_{GB}$$

We can modify the fit function

$$f(r) = \begin{cases} A[\exp\left(-(\frac{(r-2.5)}{b})\right) - \exp\left(-(\frac{(r_{min}-2.5)}{b})\right)], & r < r_{min} \\ \\ 0, & r \geq r_{min} \end{cases}$$

so that

$$A = 38.39547022 \quad \epsilon_{GB}$$

is now a reasonable number and not of the order of $\mathcal{O}(10^{22})$. We simply shifted the fit to the right.

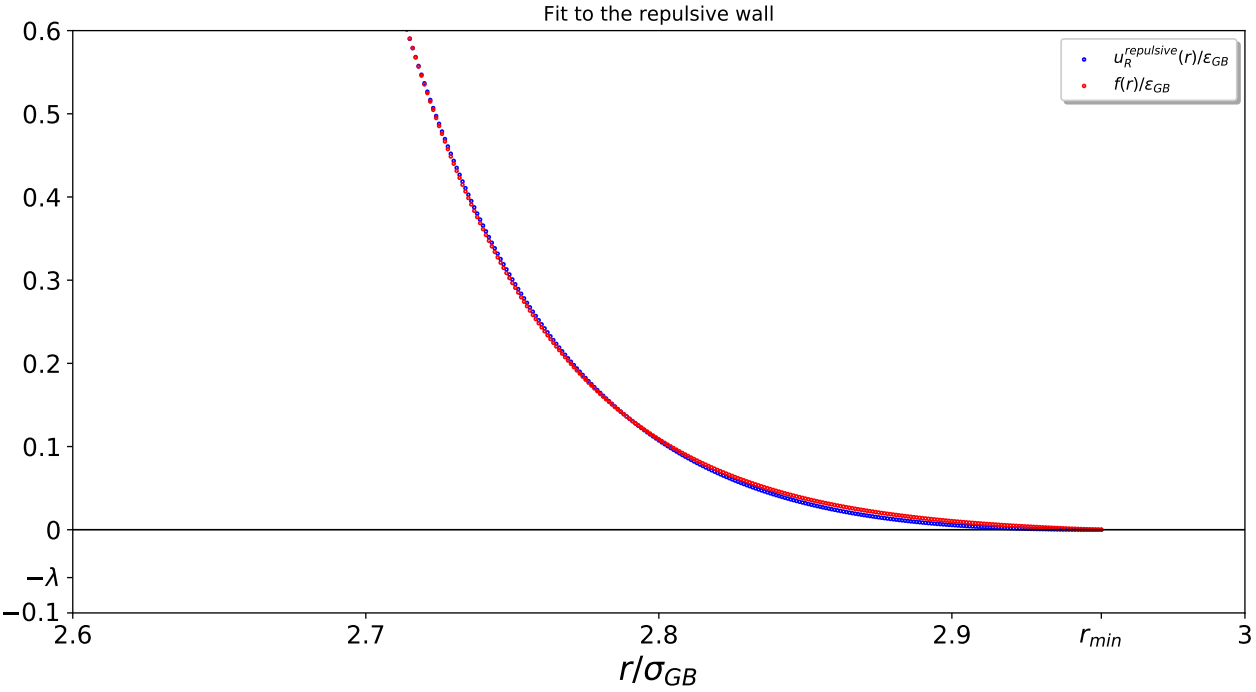

Figure 4: The repulsive wall and the fit. It seems that there is some small disagreement but a logarithmic plot will only tell.

If we take a look at the logarithmic plots of the dimensionless functions, there is disagreement

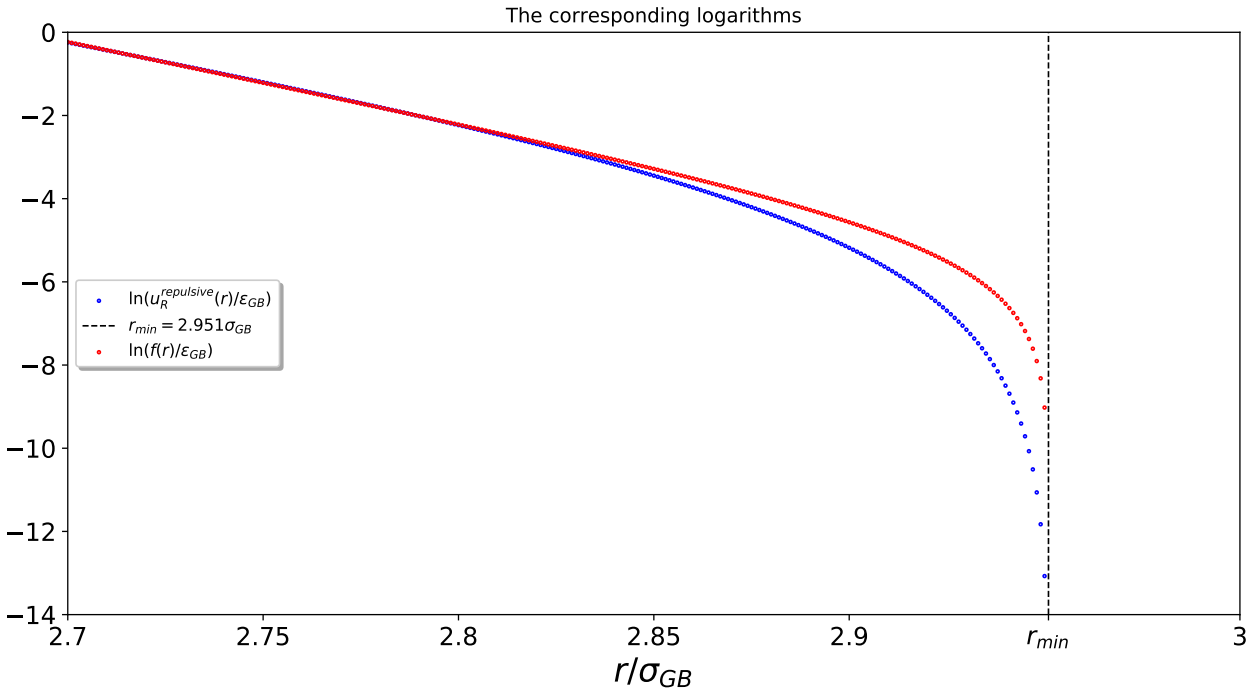

Figure 5: The corresponding logarithms so that we can magnify and compare with the eye the two functions. The disagreement is more apparent for values close to the r_{min}. I think that it will not be a problem since the discrepancy is small.

6 The pair correlation function

In order to simulate the reference system we will need the force,

$$F(r) = -\frac{df(r)}{dr} = \frac{A}{b}[\exp\left(-(\frac{(r-2.5)}{b})\right)]$$

with

$$A = 38.39547022$$

$$b = 0.0516268618$$

We will also need the thermodynamic conditions

$$\rho_R^* = 0.035648$$

$$T_R^* = 0.057524$$

$$N = 800$$

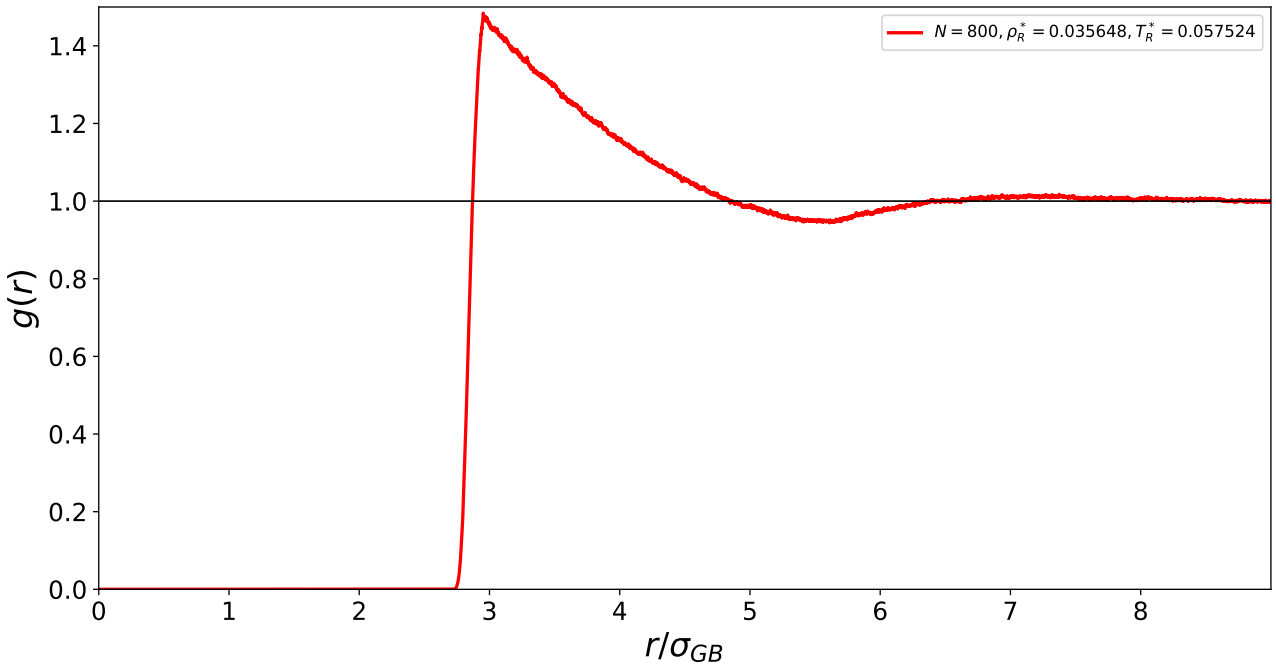

Figure 6: The pair correlation function of the reference system.

The spherical molecules are much bigger than the Gay-Berne molecules so the pair correlation function starts to rise at around $2.8275\sigma_{GB}$ which is the effective distance of the reference system molecules. We can multiply the x axis with $\frac{1}{r_{cr}}$ and compare with the Gay-Berne pair correlation function on the same scale.

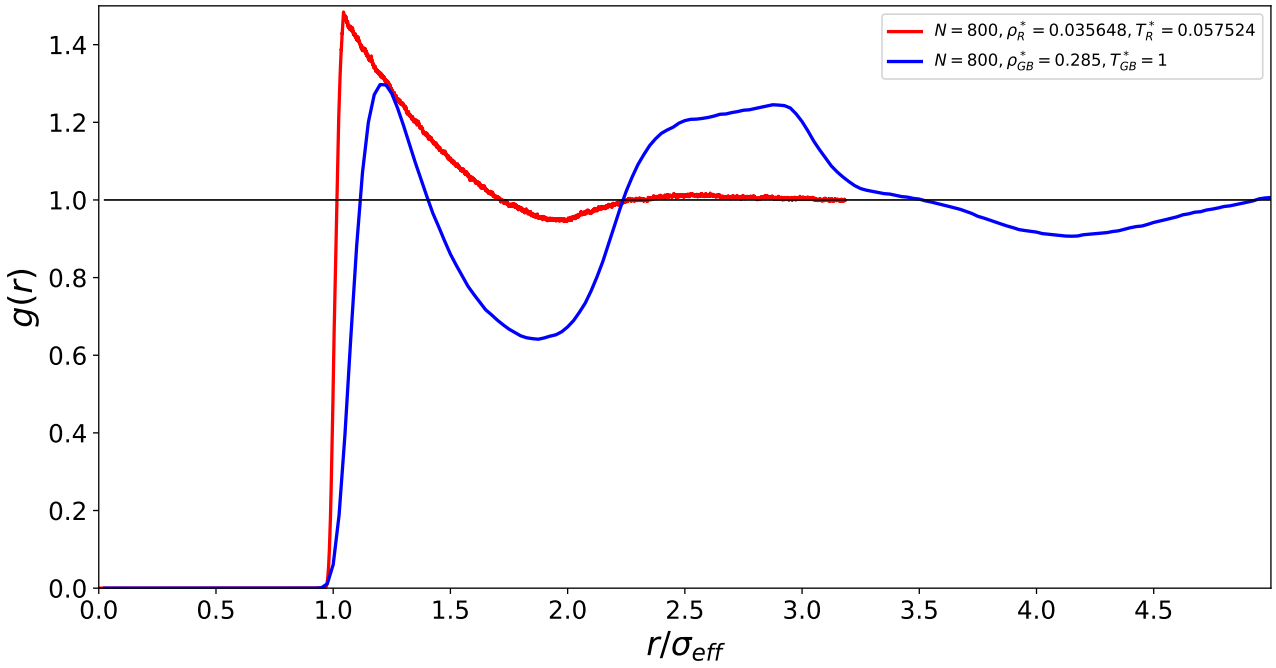

Figure 7: The comparison between the two pair correlation functions. The red one belongs to the reference system and the blue one belongs to the Gay-Berne system. For both lines I used 50,000 configurations. For both cases I got up to $r = 9$ but since I divided the r data with r_{cr} which is a little less than 3 now the red line goes a little further than 3.

7 Calculation of the c_{nn} functions

The quantity we wish to calculate is the orientational correlation parameter ϵ(See equation 1). We can write the terms of the sum explicitly to get a better idea of what we are dealing with,

$$\epsilon = -\frac{1}{8}\rho_R \int d\vec{r} \quad [2^2 g_R(r)c_{22}(r) + 4^2 g_R(r)c_{44}(r) + 6^2 g_R(r)c_{66}(r)] \tag{4}$$

where c_{nn} is defined as

$$c_{nn}(r) = \int \frac{d\hat{\Omega}_j}{2\pi} \int \frac{d\hat{\Omega}_k}{2\pi} T_n(\hat{\Omega}_j \cdot \hat{r}_{jk}) T_n(\hat{\Omega}_k \cdot \hat{r}_{jk}) u_{GB}(j,k)$$

or

$$c_{nn}(r) = \int_0^\pi \frac{d\theta_i}{\pi} \int_0^\pi \frac{d\theta_j}{\pi} \cos n\theta_i \cos n\theta_j u_{GB}(\vec{r}_{ij}, \hat{\Omega}_i, \hat{\Omega}_j)$$

We don't know how many c_{nn} functions are gonna be needed but for starters I calculated the first three functions: c_{22}, c_{44} and c_{66}. It is of most importance to see if the sum converges so I plotted the $c_{nn}(r)$ functions as they appear,

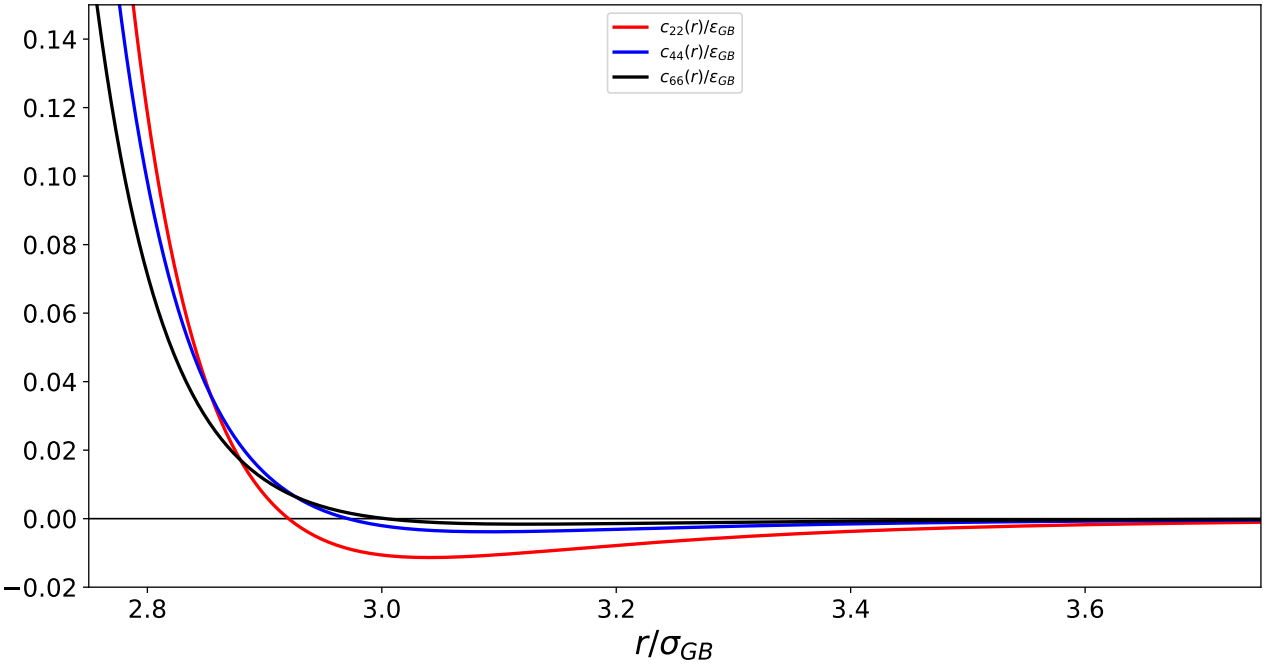

Figure 8: The three leading coefficients zoomed in the "interesting" region of $r \in [2.7, 3.7]$. The coefficients as they are actually seem to converge.

And a plot of $n^2, c_{nn}(r)$

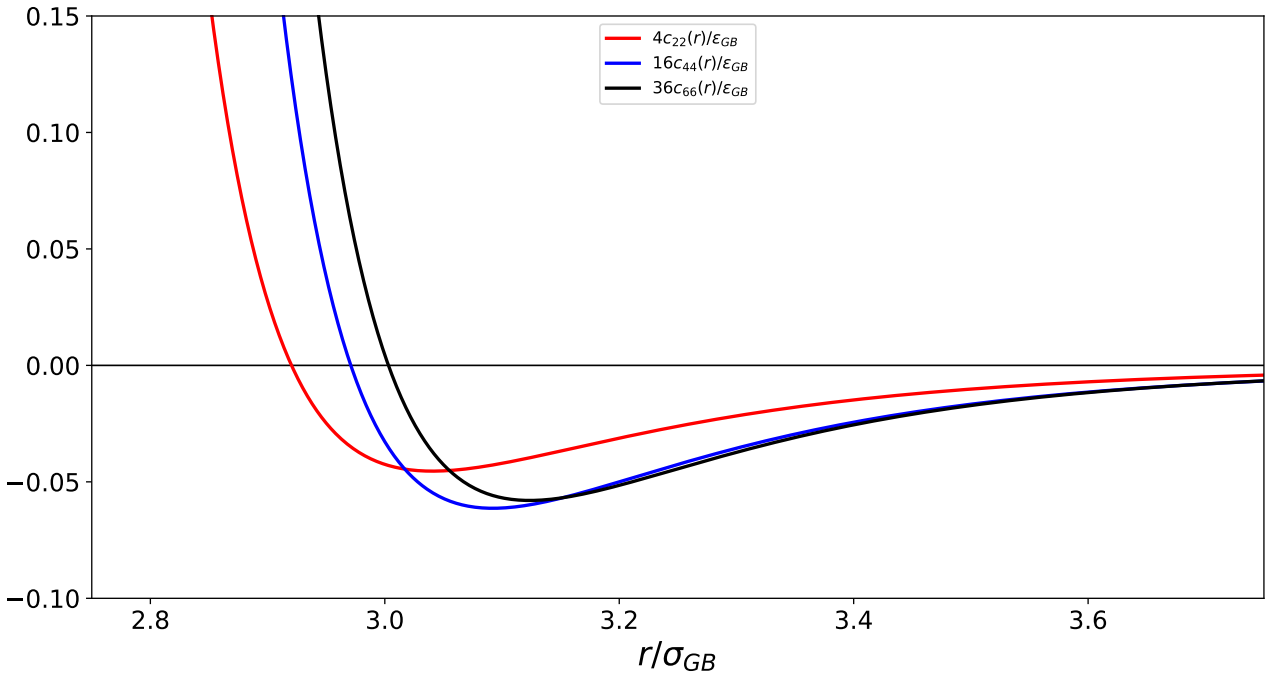

Figure 9: Now that I included the n^2 in front of the coefficients, they actually diverge. The divergence seems to happen when n^2 is included so it won't depend of the choice of $g_0(r)$.

I also plotted the terms as they appear inside the integral.

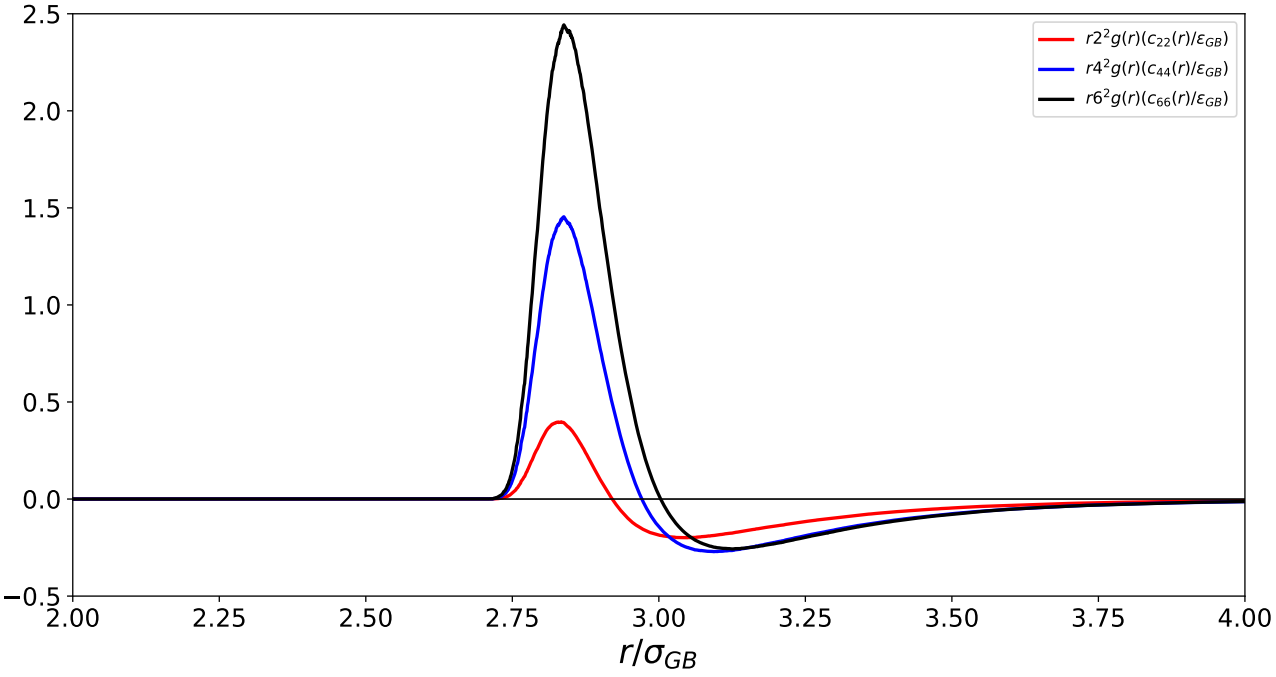

Figure 10: The three first terms in the calculation of ϵ. The terms become more important as n increases.

8 The evaluation of $\beta\epsilon$

We now have everything we need in order to calculate the orientational correlation parameter. From equation 4 we have

$$\epsilon = -\frac{2\pi}{8}\rho_R \int_0^4 dr(2^2 r g_R(r) c_{22}(r) + 4^2 r g_R(r) c_{44}(r) + 6^2 r g_R(r) c_{66}(r))$$

Through numerical integration we get,

$$\epsilon = -0.00650231\epsilon_{GB}$$

In our Large deviation/Pade scheme we make use of the dimensionless correction, $\beta\epsilon$,

$$\epsilon\beta_R = \frac{\epsilon}{k_B T_R} = \frac{-0.00650231\epsilon_{GB}}{0.057524\epsilon_{GB}} = -0.11304$$

I am not sure about the sign. The equivalent answer for the Ising model is an effective field that the designated spin feels,

$$\epsilon\beta = \beta z J m$$

which is a positive quantity ($\epsilon\beta > 0$) for a highly ordered phase ($m \to 1$). That means that the surrounding spins enhance the intensity of the magnetic field that the designated spin experiences.

9 The Pade/LDT probability distribution

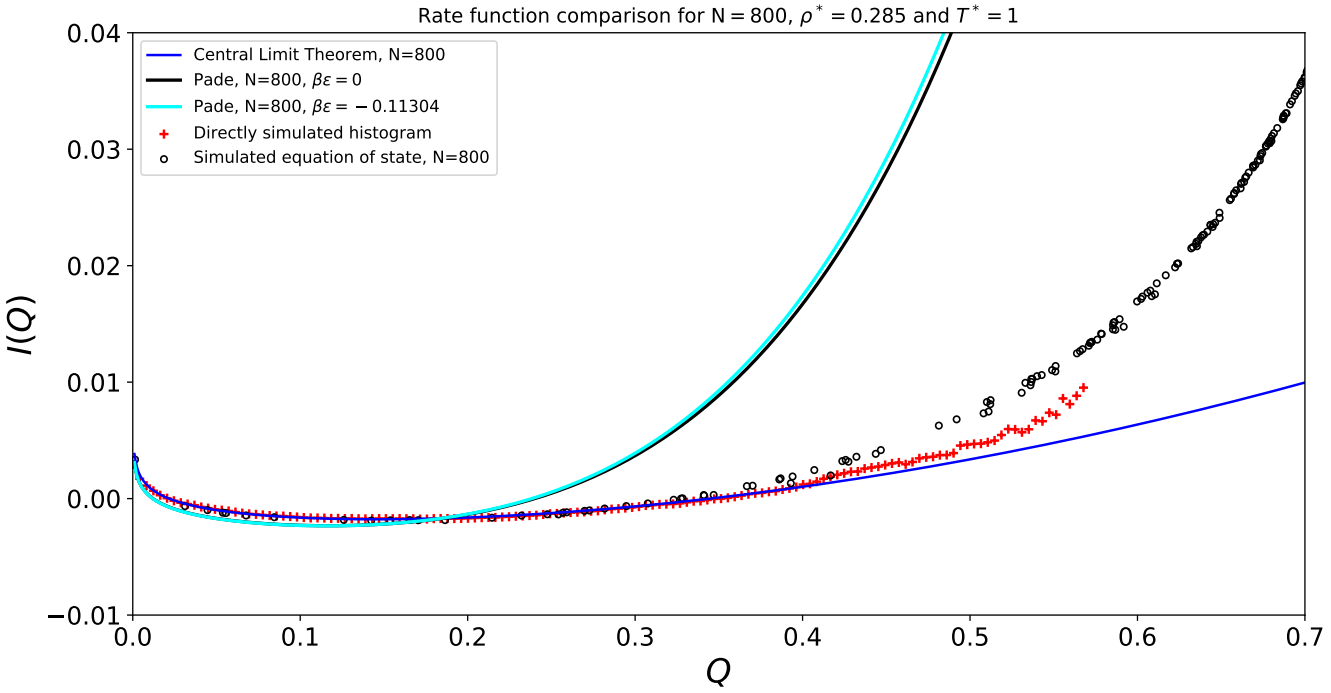

Figure 11: The comparison between rate functions in the pre-transitional isotropic phase. The blue line is the central limit theorem answer. The red dotted line is the directly simulated answer. The black dots represent the ldt approach with the simulated equation of state. The solid black curve is the ldt/Pade approach with zero mean field correction and finally the cyan curve is the ldt/Pade approach with the $\beta\epsilon$ correction.

10 The Pade formula

The disordered limit corresponds to the central limit theorem answer and the ordered limit corresponds to the uncorrelated system with the mean field correction inspired by the Ising model,

$$\gamma(Q) = \begin{cases} \frac{2}{\chi}Q + O(Q^3), & Q \to 0 \\ \\ \frac{1}{2(1-Q)} + \frac{1}{4} - \beta\epsilon, & Q \to 1 \end{cases}$$

Correlations are included in the $Q \to 0$ limit through the susceptibility χ, but in the $Q \to 1$ limit, correlations have no influence until higher order terms are included. We choose a ratio of a 5th polynomial divided by a second order polynomial,

$$\gamma_{Pade}(Q) = C\frac{Q + AQ^3 + BQ^5}{1 - Q^2}$$

From the small Q limit ($Q \to 0$) we have,

$$C = \frac{2}{\chi}$$

The conditions on the constants A and B come from the need to obey the leading uncorrelated-system $Q \to 1$,

$$1 + A + B = \frac{\chi}{2} = \frac{1}{1+\delta}$$

More specifically the coefficient B will be determined by

$$\frac{B}{2\chi} = \frac{1}{4}(\beta\epsilon + \delta - \frac{1}{2})$$

where $\delta = \frac{2}{\chi} - 1$, and

$$P(Q) \sim Q(1-Q^2)^{N/2} \exp\left(-(N\delta/2)Q^2\right) \exp\left((NB/2\chi)Q^4\right) \tag{5}$$

11 A different approach to evaluating $\beta\epsilon$

So far we have been using χ as the susceptibility and it is given by

$$\chi = \left\langle \frac{1}{N} \sum_{j,k=1}^{N} \cos 2(\theta_j - \theta_k) \right\rangle = N\langle Q^2 \rangle$$

In the 3D case Yan called this γ,

$$\gamma = \left\langle \frac{1}{N} \sum_{j,k=1}^{N} P_2(\hat{\Omega}_j \cdot \hat{\Omega}_k) \right\rangle$$

It can be calculated from the simulation. The second moment is calculated from the histogram in the following manner

$$\langle Q^2 \rangle = \sum_i p_i (\frac{Q_i + Q_{i+1}}{2})^2$$

where $p_i = \frac{n_i}{\sum_i n_i}$ is the probability, n_i represents the height of the i-th bin and Q_i represents the bin. The values we get for different system sizes do vary with N for the pre-transitional density in contrast to the isotropic phase (In the isotropic phase the susceptibility for all N is $\chi \approx 3$),

N	χ	δ
128	25.4346739488248	-0.92136718
242	30.0778557550076	-0.93350589
450	34.0865540861626	-0.94132583
800	34.2107539901964	-0.94153885

For the first moment we have a similar expression

$$\langle Q \rangle = \sum_i p_i (\frac{Q_i + Q_{i+1}}{2})$$

N	$\langle Q \rangle$
128	0.4191472629515983
242	0.3239190027100480
450	0.2498973655500179
800	0.1852011105610715

We might be able to use the first moment in order to evaluate the high limit correction, $\beta\epsilon$,

$$\langle Q \rangle = \int_0^1 Q P_{norm}(Q) dQ$$

where

$$P_{norm}(Q) = \frac{1}{C} Q(1-Q^2)^{N/2} \exp\left(-(N\delta/2)Q^2\right) \exp\left((NB/2\chi)Q^4\right)$$

with C the normalization constant calculated via gaussian quadrature,

$$C = \int_0^1 Q(1-Q^2)^{N/2} \exp\left(-(N\delta/2)Q^2\right) \exp\left((NB/2\chi)Q^4\right)$$

Of course we can get the average order parameter straight from the simulation and get the optimum $\beta\epsilon$ iteratively. Technically we will keep iterating $\beta\epsilon$ values till the absolute difference,

$$|\langle Q \rangle_{sim} - \frac{\int_0^1 Q^2(1-Q^2)^{N/2} \exp\left(-N\frac{\delta}{2}Q^2\right) \exp\left(-N(\frac{1}{8}-\frac{\delta}{4})Q^4\right) \exp\left(\frac{N}{4}\beta\epsilon Q^4\right)}{\int_0^1 Q(1-Q^2)^{N/2} \exp\left(-N\frac{\delta}{2}Q^2\right) \exp\left(-N(\frac{1}{8}-\frac{\delta}{4})Q^4\right) \exp\left(\frac{N}{4}\beta\epsilon Q^4\right)}| < \alpha_N$$

is a tiny number α_N. We can name the second term $\langle Q \rangle_{num}$ and make a plot of the absolute difference versus the mean field correction,

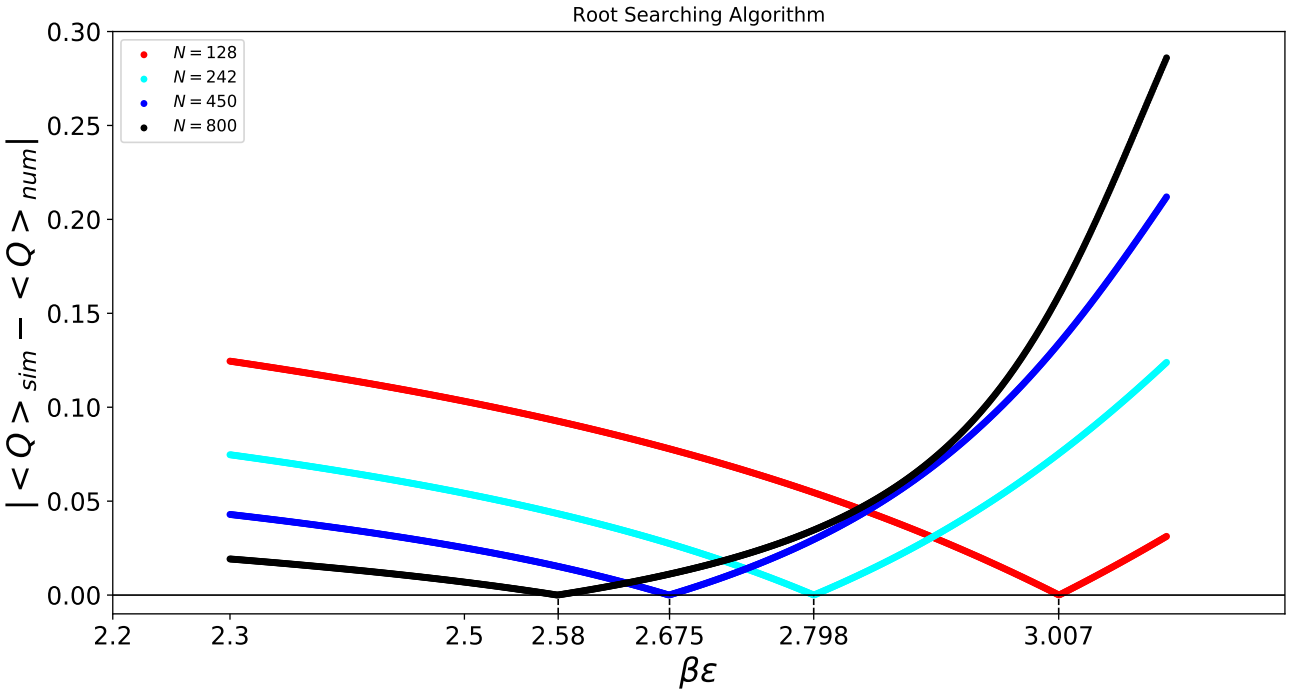

Figure 12: The root searching algorithm that was used for the four N values of interest.

I chose $\beta\epsilon$ increments of 0.001 and decided to stop when the difference α_N becomes of the order of 10^{-5}. In the form of a table we have,

N	$\beta\epsilon$	α_N
128	3.007	8.9×10^{-5}
242	2.798	3.1×10^{-5}
450	2.675	8.8×10^{-5}
800	2.580	6.7×10^{-5}

We can now go back to the N-scaling studies and use the mean field corrections for each system size. First of all let's plot the different curves in the pre-transitional isotropic region WITHOUT the correction

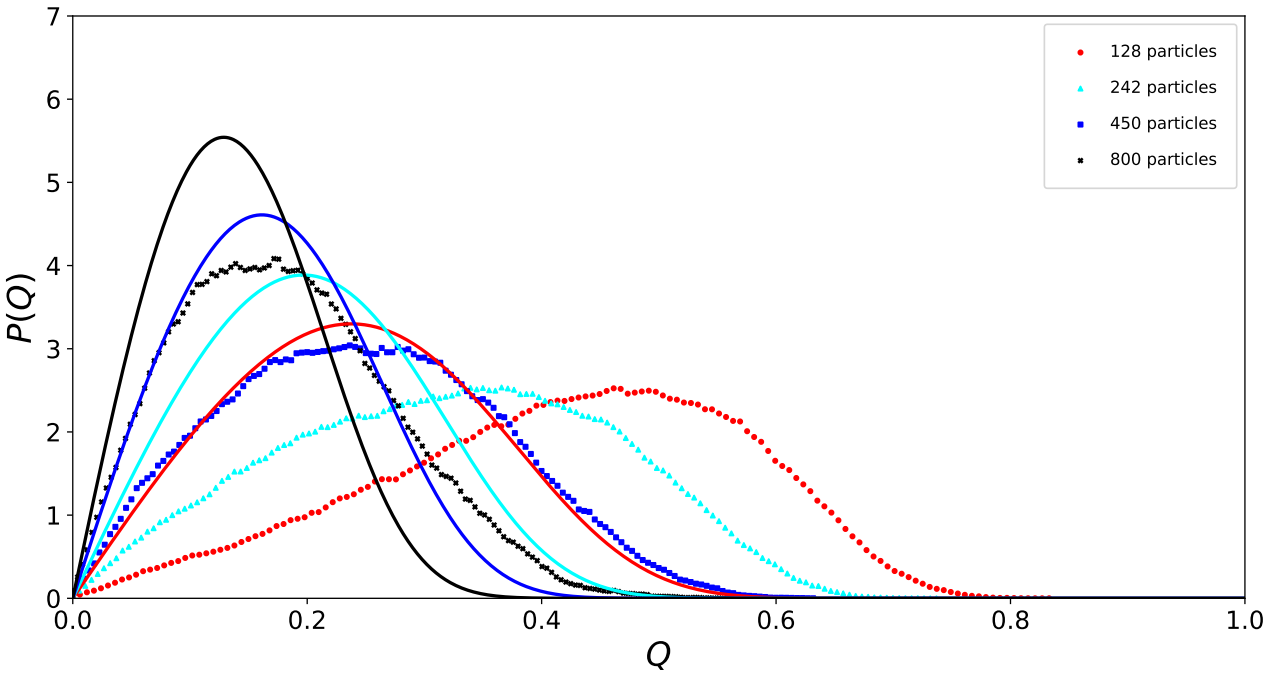

Figure 13: N scaling in the pre-transitional isotropic phase, ($\rho^* = 0.285$ - $T^* = 1$). Solid curves are the Pade' predictions with no mean field correction ($\beta\epsilon = 0$ for every value of N). Dots represent the histograms where the number of bins is 140 and the number of configurations is 10^7.

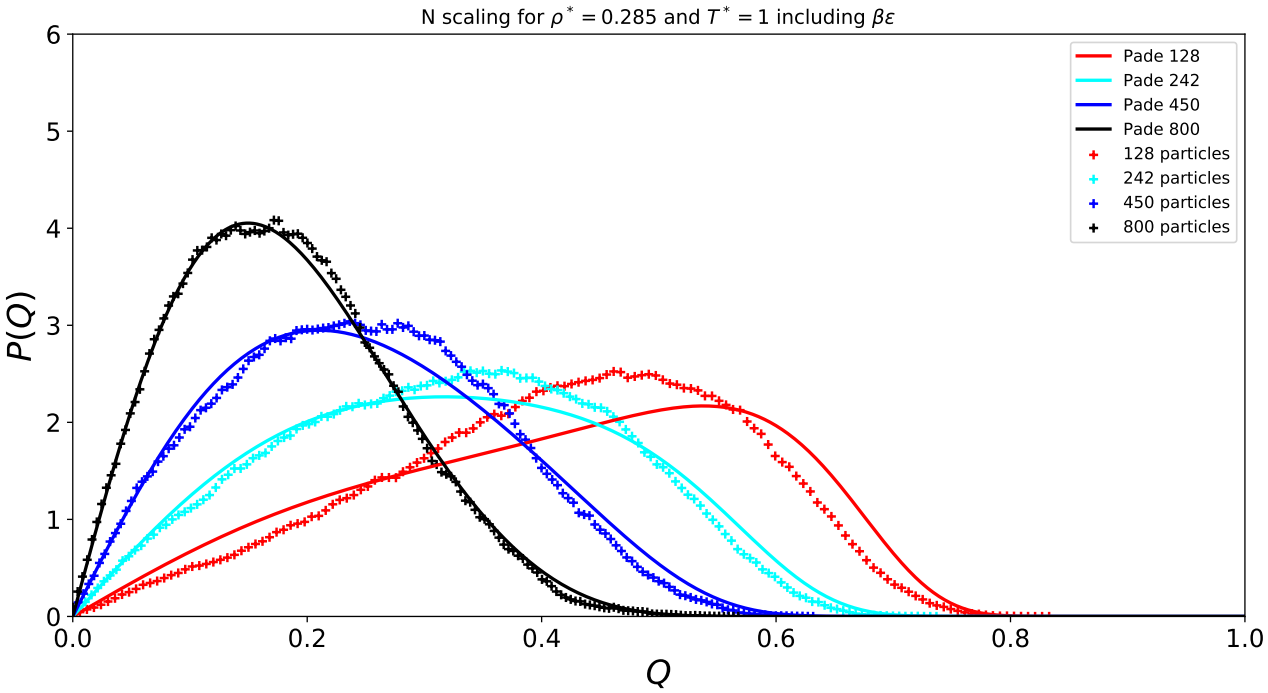

Figure 14: The same graph as the previous figure but with the mean field correction included, $\beta\epsilon \neq 0$ for every value of N. The difference is stunning. The only system that deviates is the small system and it could be because of difficulty to relax.

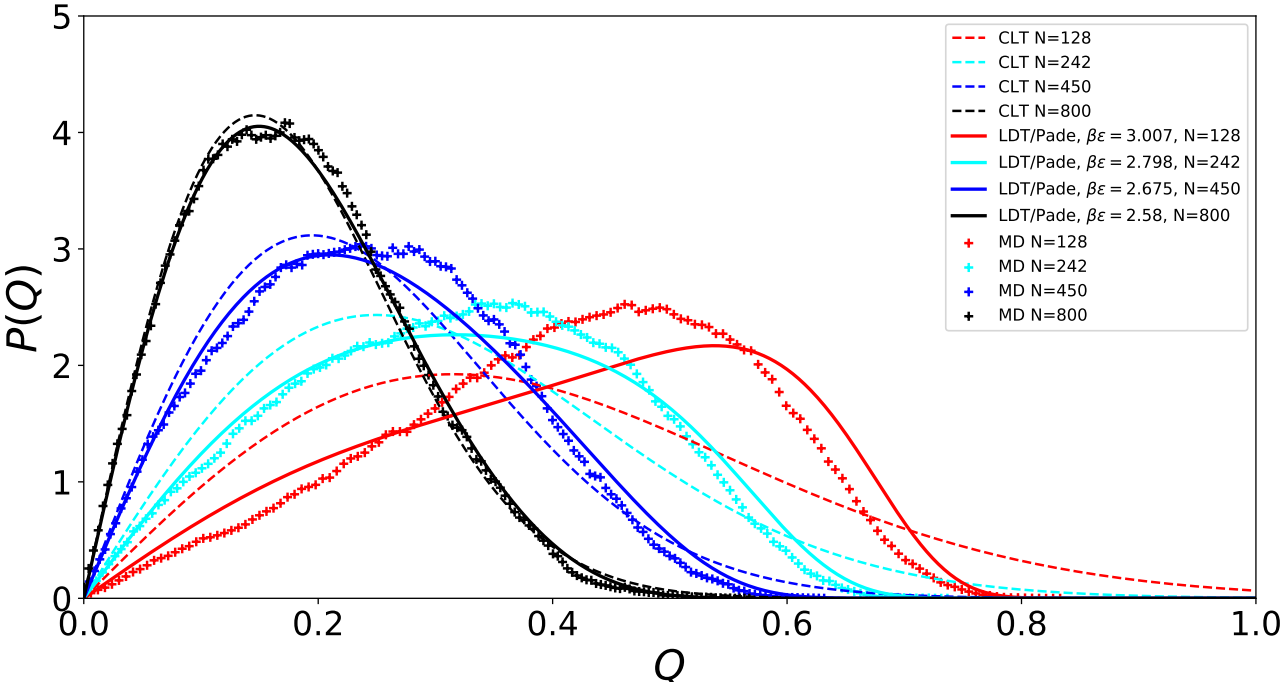

Figure 15: The LDT/Pade scheme captures the finite size scaling of the system more accurately than the CLT approach.

It is difficult to see the N-scaling from that involved graph so it makes sense to plot the probability distributions separately for each N starting with $N = 800$.

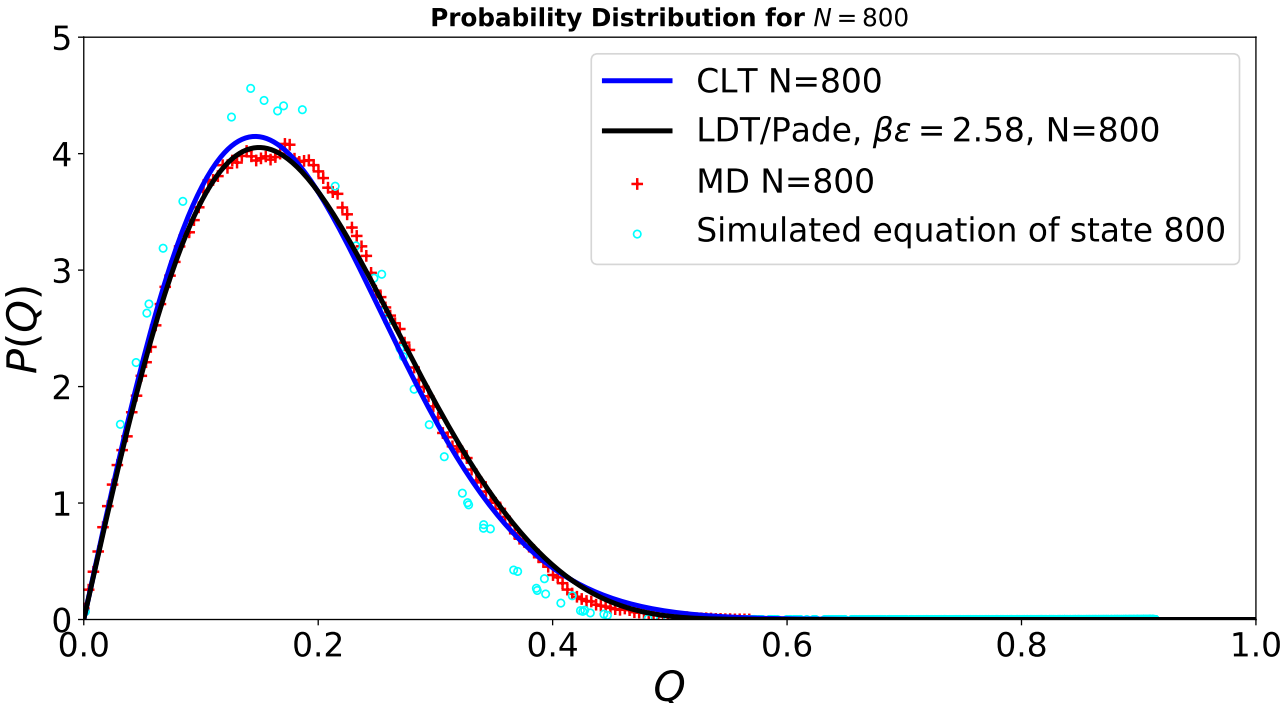

Figure 16: Probability distributions for the largest system we have studied so far in the two dimensional case.

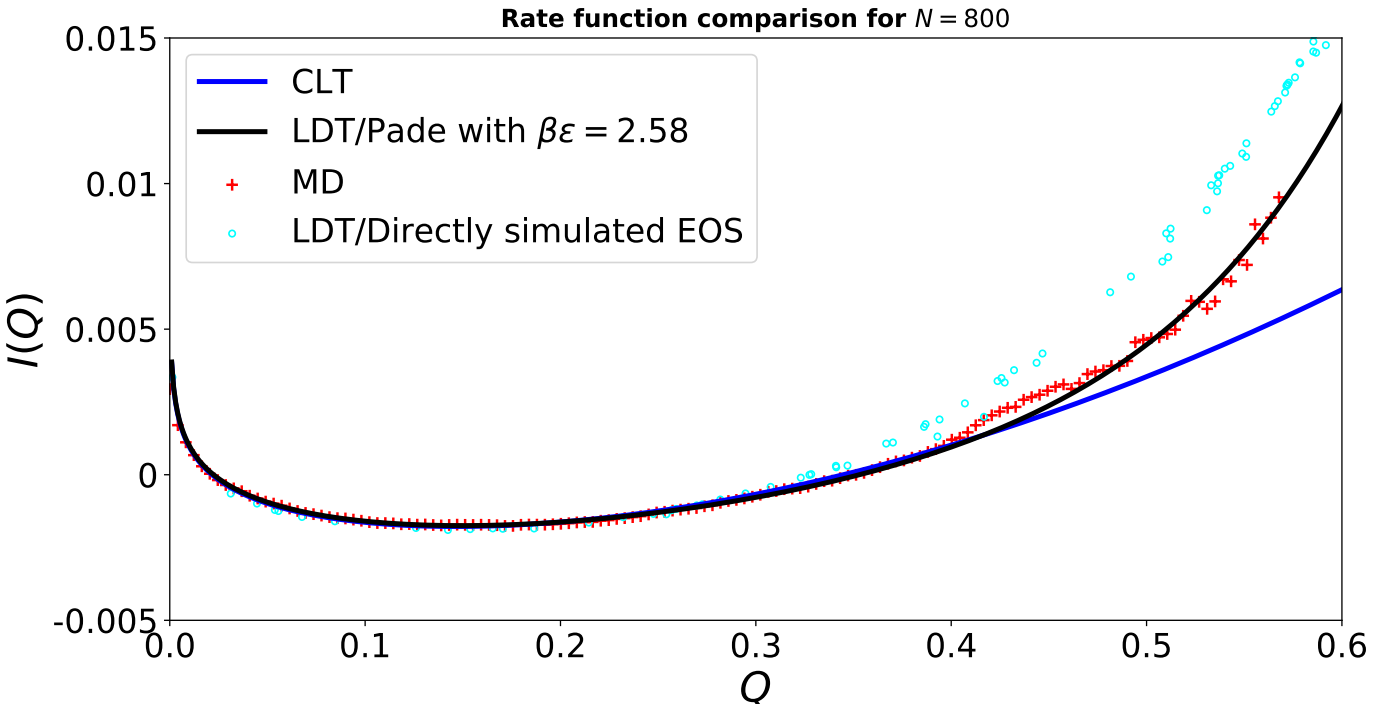

Figure 17: This is a comparison between the rate functions of the different approaches for the $N = 800$ system. Good agreement between all the different approaches for small deviations around the minimum value of the rate function as expected. Obvious disagreement for larger deviations. The LDT/Pade scheme successfully describes the behavior observed in the simulation. I think this is the very first value that N is sufficiently big enough to make LDT a very strong predictor of large values of Q.

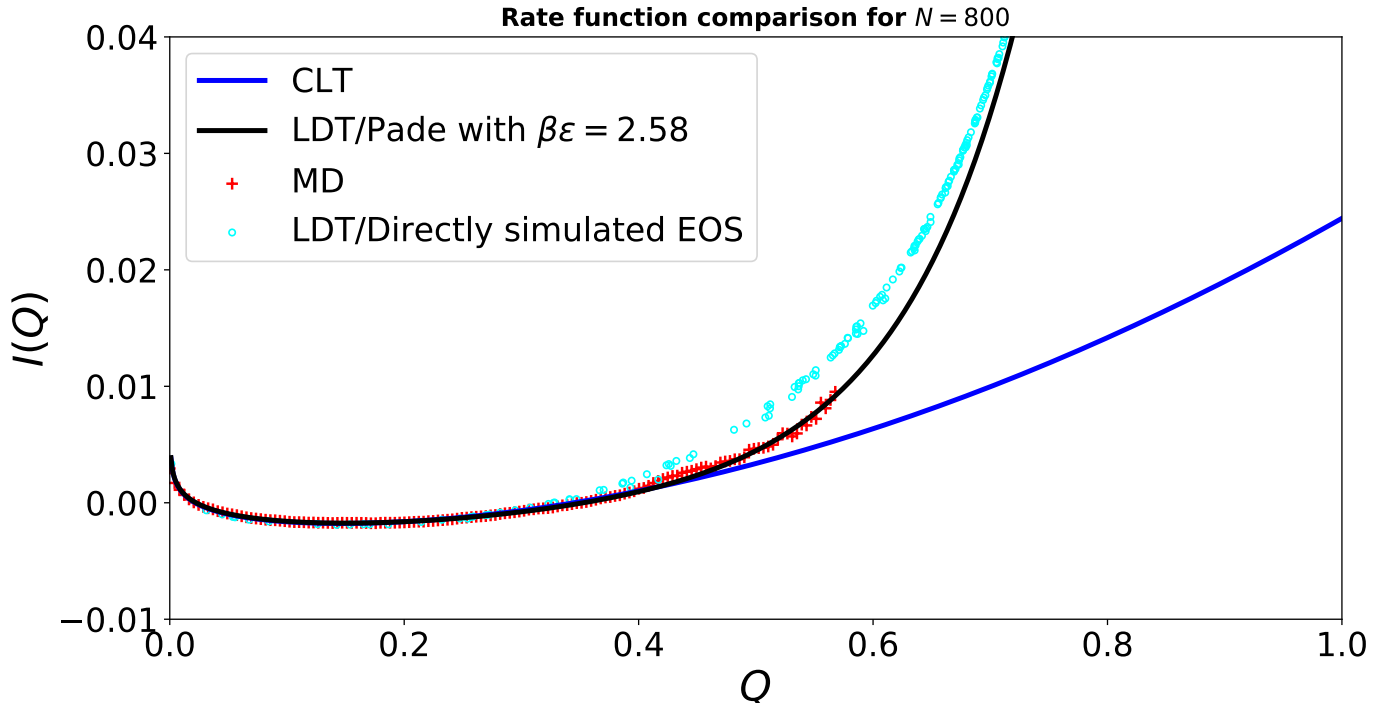

Figure 18: Same graph but I zoomed out in order to show the lines in the full Q range.

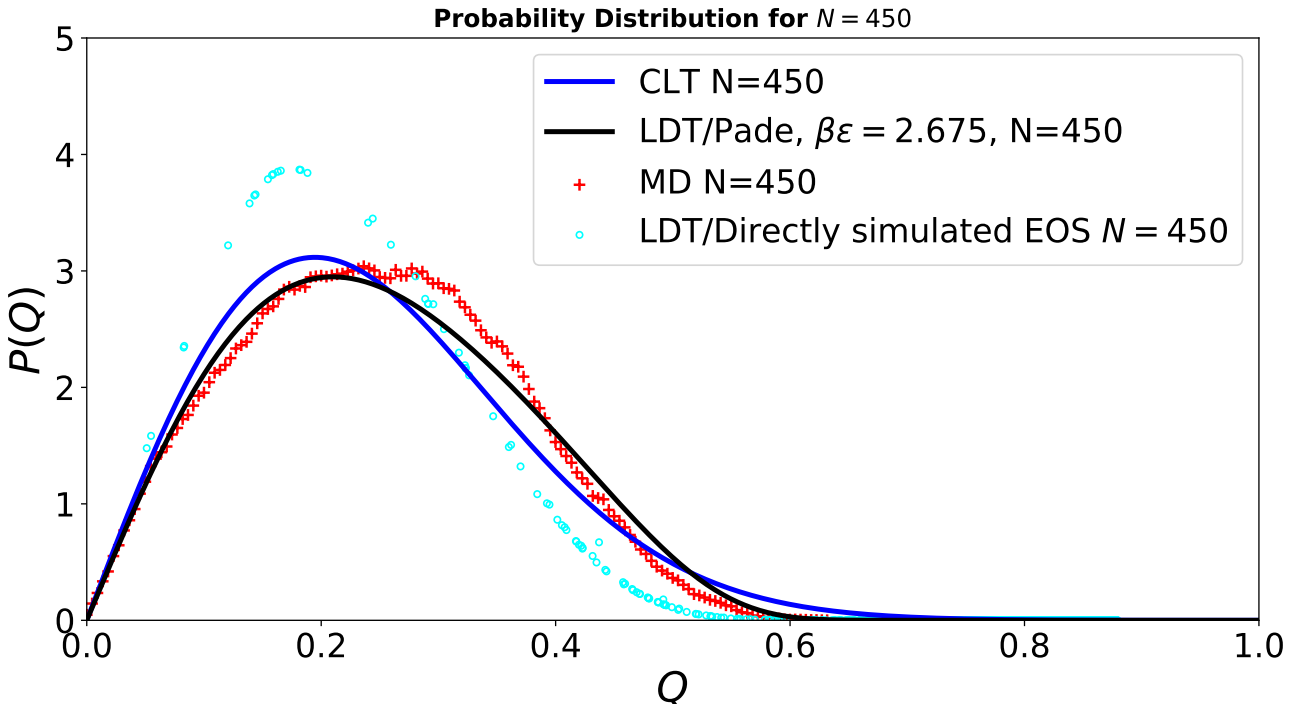

Figure 19: The probability distribution for $N = 450$.

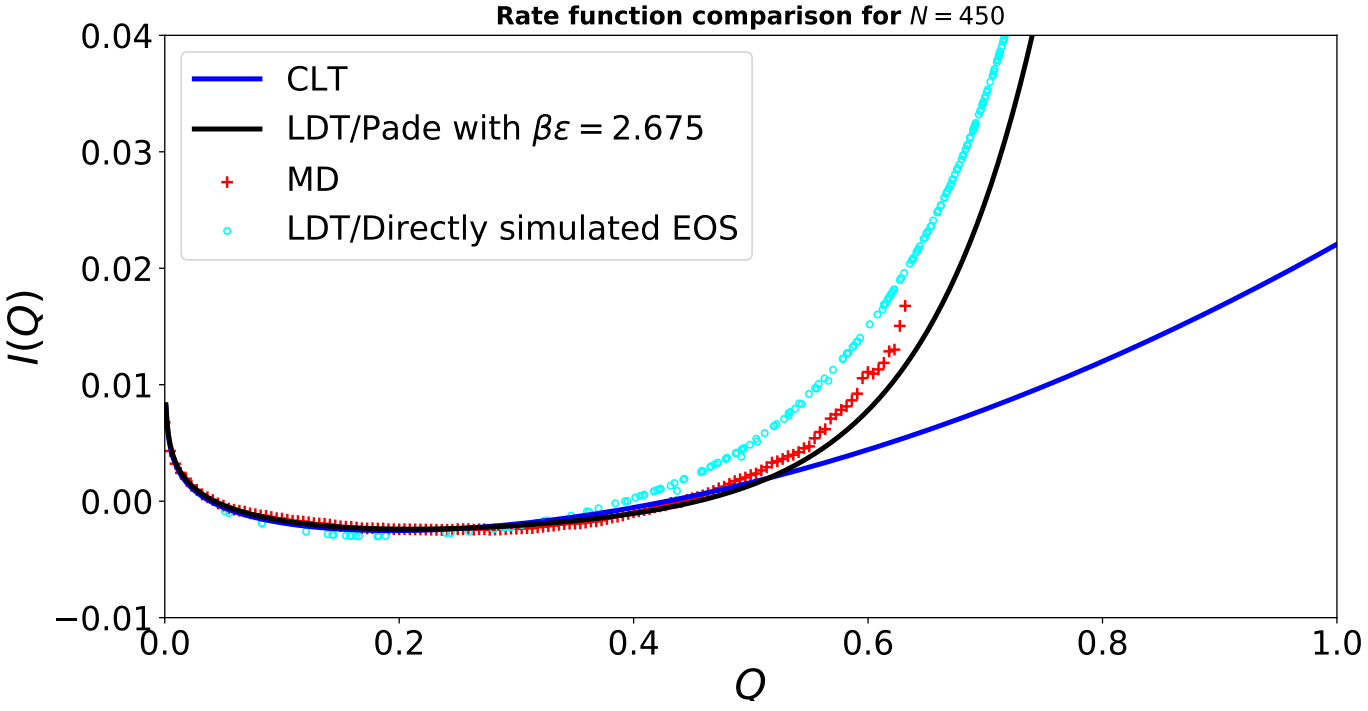

Figure 20: This is a comparison between the rate functions of the different approaches for the $N = 450$ system.

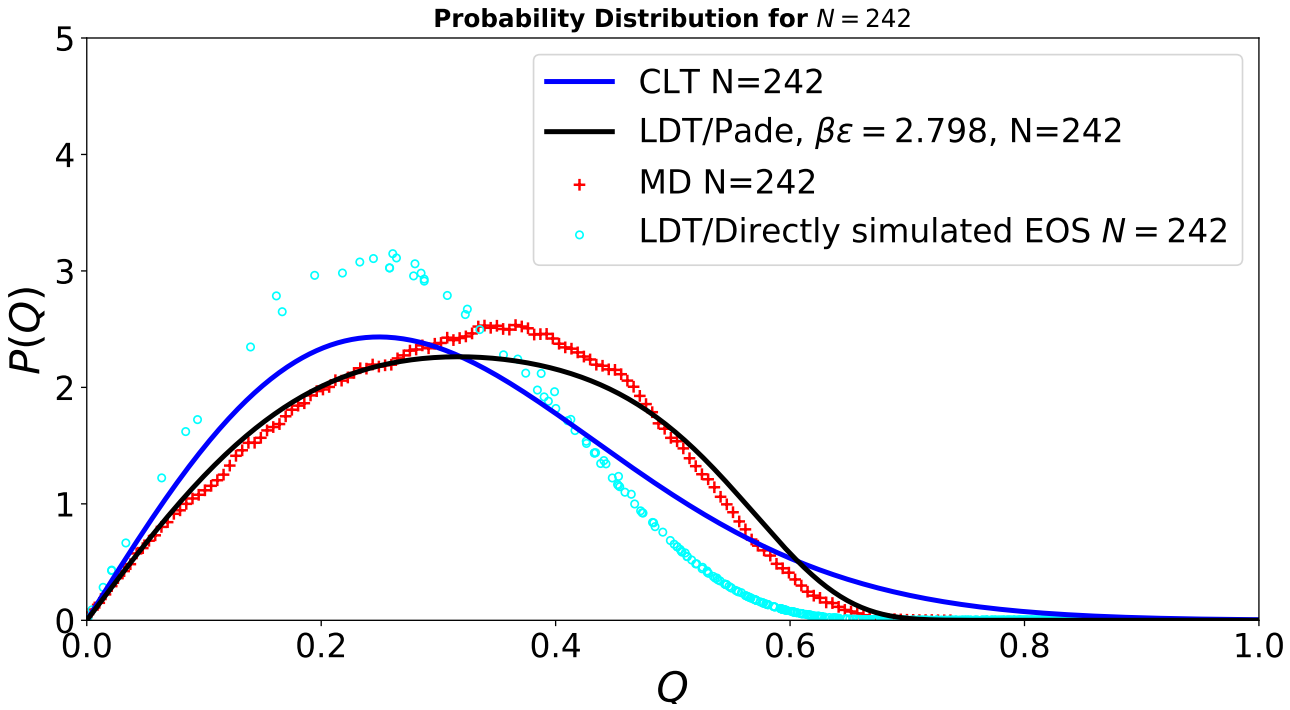

Figure 21: The probability distribution for the $N = 242$ case.

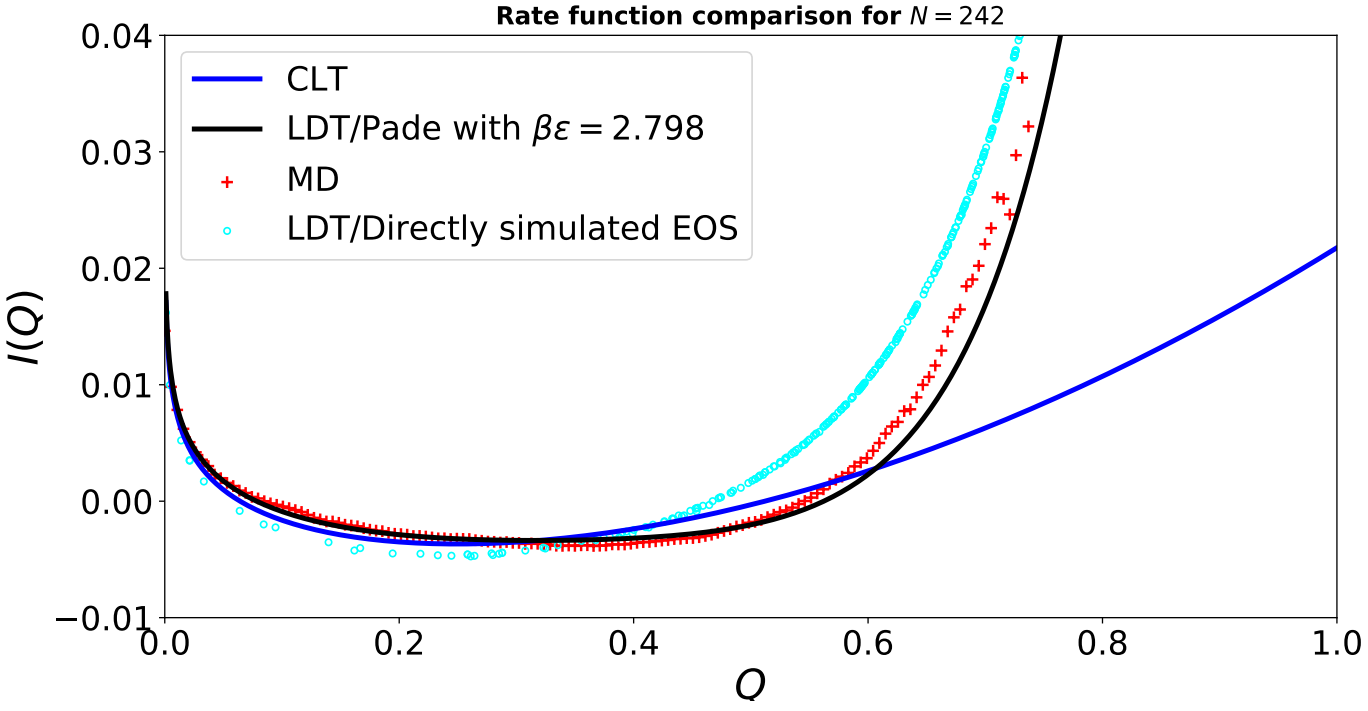

Figure 22: Comparison between the rate functions of the different approaches for the $N = 242$ system.

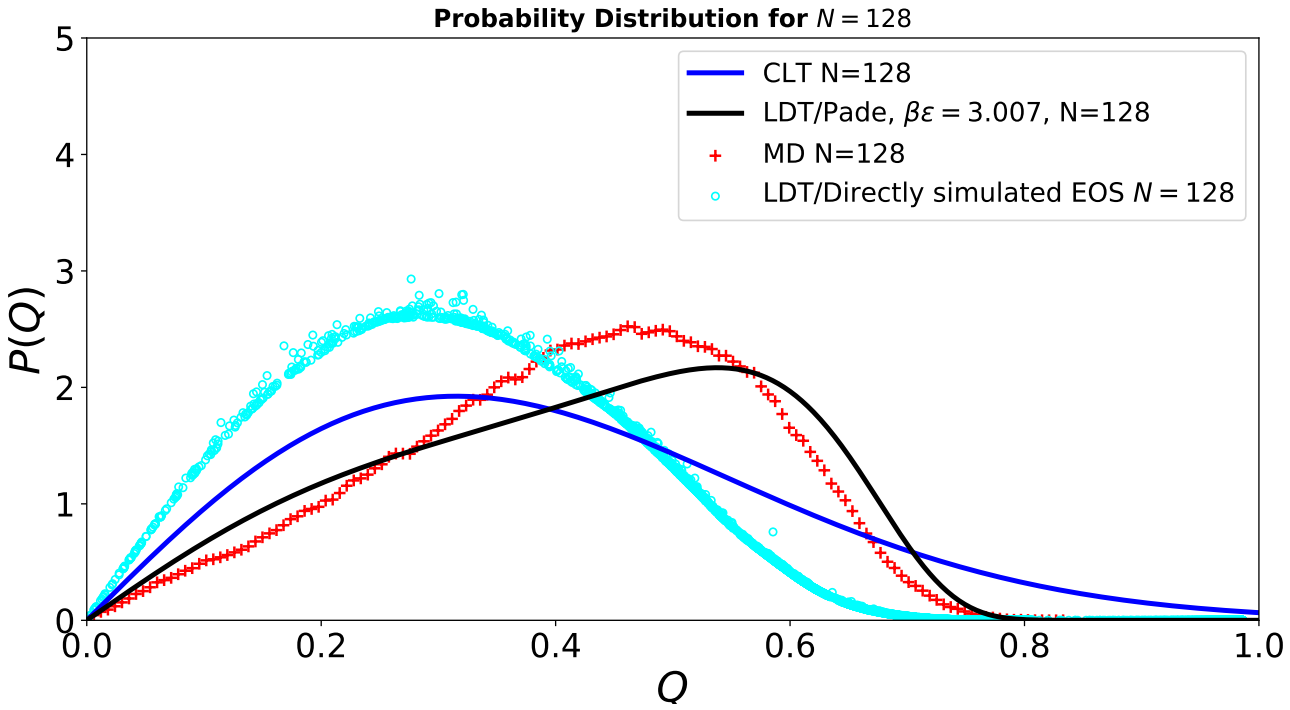

Figure 23: The probability distributions for the smallest system we have studied so far, $N = 128$.

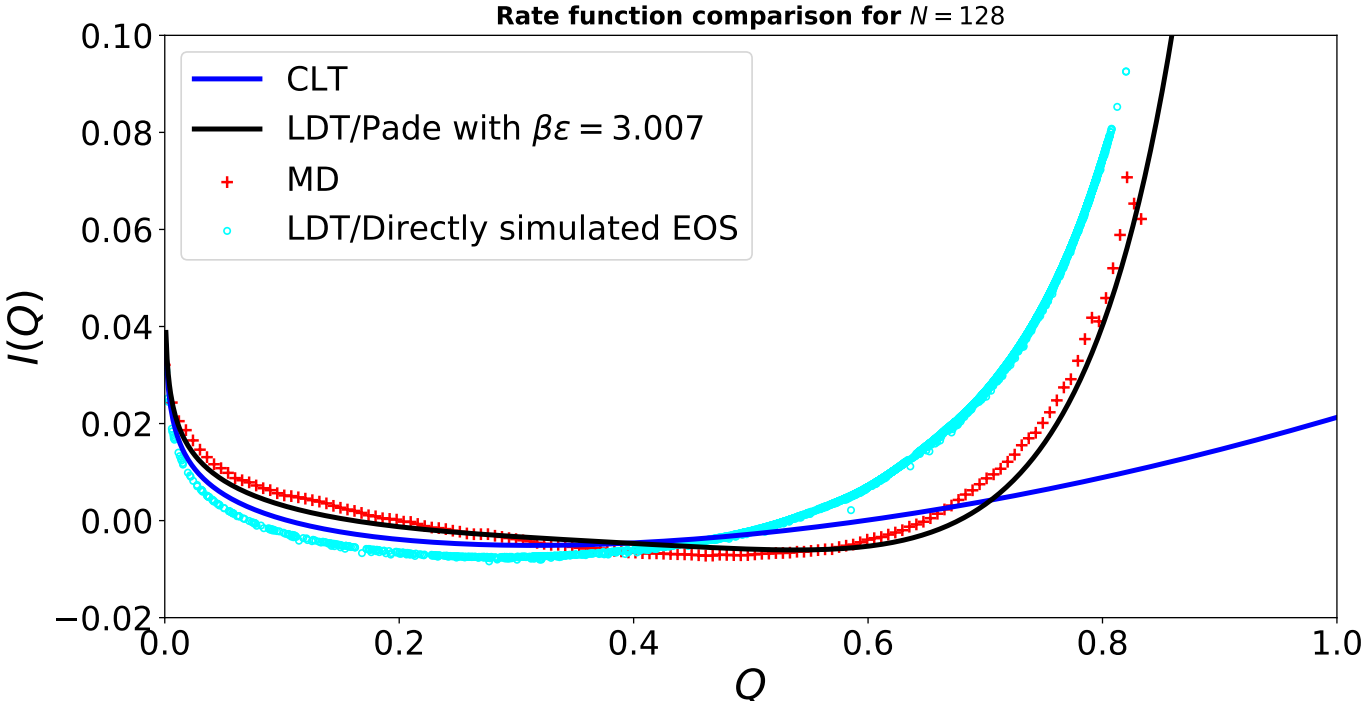

Figure 24: A final comparison between the rate functions of the different approaches for the $N = 128$ system.

12 Finite size scaling by looking at the average value only

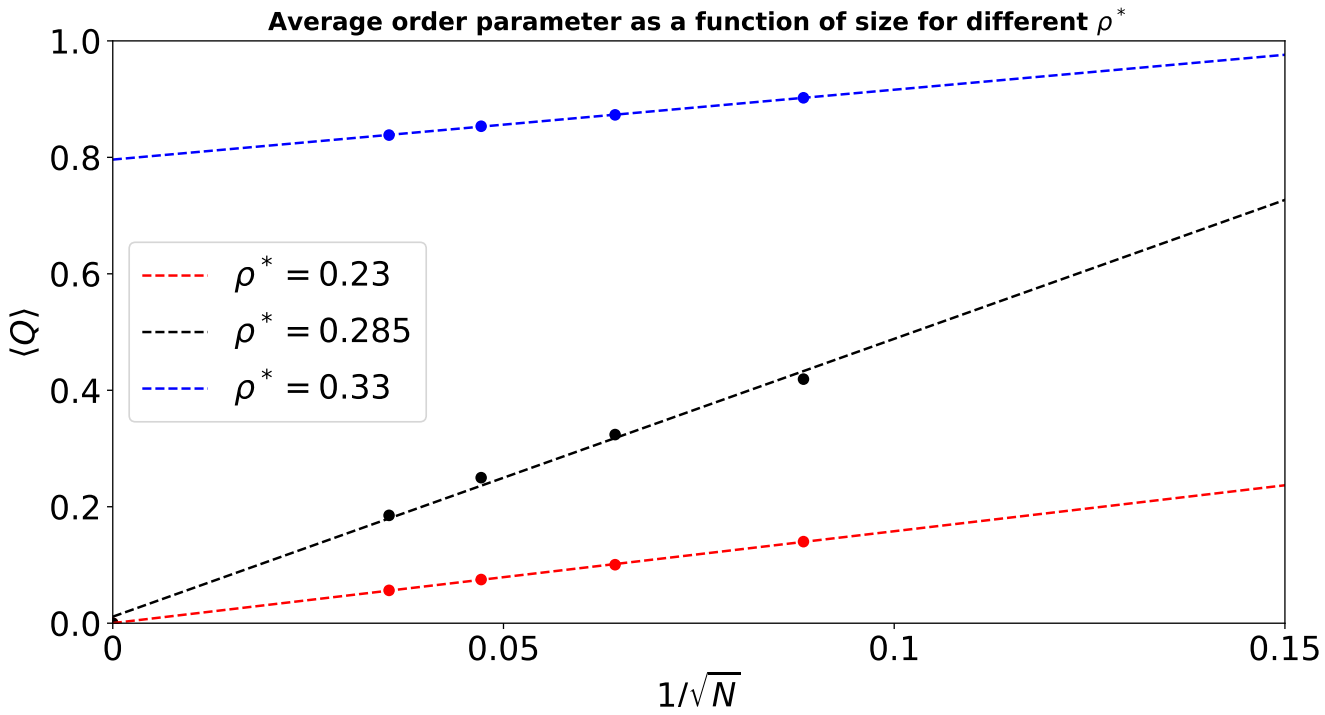

Figure 25: Finite-size scaling behavior of $\langle Q \rangle$, the average value of the orientational order parameter Q for three different densities, ρ^*. We expect the nematic order to drop in the thermodynamic limit due to the Mermin Wagner theorem. If the authors of Kundu et al. (2021) are correct, then we would expect the long range orientational order to diminish as we go to bigger and bigger systems. Finally we would expect it to drop to zero in the thermodynamic limit. In order to formally prove it for our GB(3,5,2,1) model we need to simulate bigger N nematic systems and calculate the average order parameter and at least observe the straight line to start to curve downwards.

References

P. Kundu, J. Saha, and P. Mishra. Long-range decay of pair correlations and nematic ordering in a two-dimensional system of gay-berne mesogens. *Fluid Phase Equilibria*, 549:113224, 2021. ISSN 0378-3812. doi: https://doi.org/10.1016/j.fluid.2021.113224. URL https://www.sciencedirect.com/science/article/pii/S0378381221002879.